INVITED COMMENT

Thermal baths as quantum resources: more friends than foes?

To cite this article: Gershon Kurizki *et al* 2015 *Phys. Scr.* **90** 128002

View the article online for updates and enhancements.

Related content

- PhD Tutorial
  Goren Gordon

- Direct measurement of the system-environment coupling as a tool for understanding decoherence and dynamical decoupling
  Ido Almog, Yoav Sagi, Goren Gordon et al.

- Experimental investigations of dipole–dipole interactions between a few Rydberg atoms
  Antoine Browaeys, Daniel Barredo and Thierry Lahaye

Recent citations

- Nonconservative Forces via Quantum Reservoir Engineering
  Shanon L. Vuglar *et al*

- Bath correlation functions for logarithmic-like spectral densities
  Filippo Giraldi

- Criticality of environmental information obtainable by dynamically controlled quantum probes
  Analia Zwick *et al*

Invited Comment

Thermal baths as quantum resources: more friends than foes?

Gershon Kurizki[1]**, Ephraim Shahmoon**[2] **and Analia Zwick**[1]

[1] Weizmann Institute of Science, Rehovot 76100, Israel
[2] Department of Physics, Harvard University, Cambridge MA 02138, USA

Abstract

In this article we argue that thermal reservoirs (baths) are potentially useful resources in processes involving atoms interacting with quantized electromagnetic fields and their applications to quantum technologies. One may try to suppress the bath effects by means of dynamical control, but such control does not always yield the desired results. We wish instead to take advantage of bath effects, that do not obliterate 'quantumness' in the system-bath compound. To this end, three possible approaches have been pursued by us. (i) Control of a quantum system faster than the correlation time of the bath to which it couples: such control allows us to reveal quasi-reversible/coherent dynamical phenomena of quantum open systems, manifest by the quantum Zeno or anti-Zeno effects (QZE or AZE, respectively). Dynamical control methods based on the QZE are aimed not only at protecting the quantumness of the system, but also diagnosing the bath spectra or transferring quantum information via noisy media. By contrast, AZE-based control is useful for fast cooling of thermalized quantum systems. (ii) Engineering the coupling of quantum systems to selected bath modes: this approach, based on field–atom coupling control in cavities, waveguides and photonic band structures, allows one to drastically enhance the strength and range of atom–atom coupling through the mediation of the selected bath modes. More dramatically, it allows us to achieve *bath-induced entanglement* that may appear paradoxical if one takes the conventional view that coupling to baths destroys quantumness. (iii) Engineering baths with appropriate non-flat spectra: this approach is a prerequisite for the construction of the simplest and most efficient quantum heat machines (engines and refrigerators). We may thus conclude that often thermal baths are 'more friends than foes' in quantum technologies.

Keywords: quantum control, open quantum systems, quantum information, quantum thermo-dynamics, quantum Zeno effect, quantum metrology, quantum entanglement

(Some figures may appear in colour only in the online journal)

1. Introduction

In this article we wish to *'make out a case'* for thermal reservoirs (baths) as potentially useful resources in quantum optics [1], namely, in processes involving matter interacting with quantized electromagnetic fields, and their applications to quantum technologies: quantum information processing [2–4], quantum sensing and metrology [5–9], as well as quantum thermodynamics [10–12]. In general, there is little we can do to avoid the ubiquitous presence of environments described as thermal baths in contact with quantum systems: with very few exceptions, all quantum systems are open [13, 14]. One may try to reduce the bath effects on the quantum system of interest by means of dynamical control, originally developed to suppress bath-induced decoherence or dissipation [15–21]. Yet such control does not always yield the desired results, hence we wish to advocate a different strategy that may be colloquially summarized as follows: *'if you can't fight the bath–join it'*, namely, take advantage of its effects, particularly those that do not obliterate 'quantumness'

in the system-bath compound. To this end, three possible approaches may be pursued, to be discussed in the subsequent sections[3]:

- **Control a quantum system** faster than **the correlation (memory) time of the bath to which it couples**: such control allows us to reveal quasi-reversible/ coherent dynamical phenomena of quantum open systems, manifest by the quantum Zeno or anti-Zeno effects (QZE or AZE, respectively) [28–33]. Dynamical control methods based on the QZE are aimed at protecting the quantumness of the system [30, 33–47], but also diagnosing the bath spectra and transferring quantum information via noisy media (section 2). By contrast, AZE-based control is useful for fast cooling of thermalized quantum systems [48–50] (section 5).
- **Engineer the coupling of quantum systems to selected bath modes**: this approach, based on field–atom coupling control in cavities [51–53] and photonic band structures [54–59], allows one to drastically modify bath-mediated exchange of virtual quanta between quantum systems and thereby enormously enhance their coupling [60–62]. Not less dramatically, such engineering allows us to achieve bath-induced entanglement [63–70] that may appear paradoxical if one takes the conventional view that coupling to baths destroys quantumness [13, 14] (sections 3–4).
- **Select or engineer baths with appropriate non-flat spectra**: this approach is a prerequisite for the construction of the simplest and most efficient quantum heat machines (engines and refrigerators) [71–73] and for investigating their ability to attain the absolute zero [73] (section 6).

Our conclusions and outlook to forthcoming research along the discussed lines are presented in section 7.

2. Control within the bath memory-time: Zeno and anti-Zeno dynamics

Our theory of quantum systems whose weak interaction with thermal baths is dynamically controlled [30, 34, 40, 42, 44, 74–76] treats all kinds of such control, be it coherent or projective (non-unitary), continuous or pulsed, as generalized forms of two generic effects or control paradigms. One is

Minimized bath effect ≡ Quantum Zeno effect (QZE),

which *minimizes* (under constraints on the control energy) the integral product (overlap) of two functions: $G(\omega)$, the coupling spectrum of the bath (obtained by Fourier-transforming its autocorrelation function) and a spectral 'filter' function $F_t(\omega)$ determined by the control field-intensity spectrum and its time duration t. It is the 'filter' function that provides the control handle on our ability to optimally execute

a desired task in the presence of a given bath. In the presence of several baths (a common situation), both $G(\omega)$ and $F_t(\omega)$ functionals are represented by matrices [74–76].

QZE-based control is required in operational tasks related to quantum information its storage and transmission [77–81], where bath effects are detrimental and must be suppressed. Regardless of the chosen form of control, the controlled-system dynamics must then be *Zeno-like*, namely, resulting in suppressed system–bath interaction.

The alternative paradigm is

Maximized bath effect ≡ Anti − Zeno effect(AZE),

which amounts to *maximized overlap* of $G(\omega)$ and $F_t(\omega)$ (under control-energy constraints, as for QZE). AZE-based control is instrumental for non-unitary operations that entail changes of the system's entropy. Such operations benefit from efficient interaction with a bath for their execution. Examples are measurements used to cool (purify) a quantum system [50], equilibrate (thermalize) it with a bath [49, 75], or harvest energy from the bath. If the underlying dynamics is anti-Zeno-like [29, 48], system–bath interaction will be enhanced and will thereby facilitate these tasks.

Certain tasks may involve state transfer or entanglement via the bath, which require maximized bipartite coupling, but minimized single-partite coupling with the bath [43, 74, 82, 83]. For such tasks, a more subtle interplay of Zeno and anti-Zeno dynamics may be optimal and depend on the quantum statistics of the bath [84].

We have therefore developed a general approach that allows one to optimize the interaction of a quantum system with the environment so as to execute a given operation, be it non-unitary or unitary, such as state-transfer or storage with maximized fidelity, purification/entropy-minimization, entanglement distribution, or energy transfer [75, 76]. This approach consists in designing the temporal dependence of the Hamiltonian that governs the system by variational minimization or maximization (as the case may be) of a state-dependent functional chosen to quantify the success probability of the operation. To this end, the temporal control must be faster than the bath correlation time [38, 75, 76]. This approach not only provides protection from adverse effects of the bath, namely, quantum-state decoherence, but actually benefits from the system–bath interactions for the realization of a given non-unitary task. More formally, it maximizes the fidelity of any given quantum operation on a multi-dimensional Hilbert space for the baths or noise sources at hand. Its main merit is that it is not restricted to pulsed forms of control, and therefore can drastically reduce the energy required to execute a task by resorting to a smoothly varying field, thereby reducing the errors incurred by control [75].

2.1. Control for bath diagnostics

We shall discuss applications of dynamical control of the system–bath coupling that go beyond its conventional use as a means of fighting decoherence [15–21, 34, 38–40, 85]. The first application of such control is as a tool of bath-spectrum diagnostics. Such diagnostics has the goal of revealing the

---

[3] Cooperative (Dicke) effects mediated by the bath are outside the scope of this article—see the following articles [22–27].
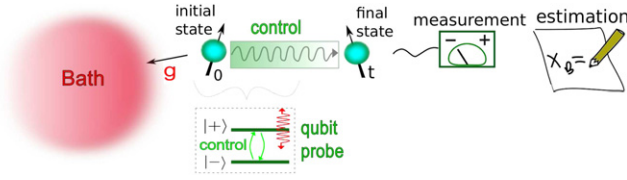
Figure 1. Schematic view of probing bath parameters by a qubit that undergoes bath-induced decoherence while being subject to dynamical control. Information on the bath that yields estimation of its parameters is extracted from a measurement of the qubit in the $|\pm\rangle = \frac{1}{\sqrt{2}}(|\uparrow\rangle \pm |\downarrow\rangle)$ basis of equation (2).

dynamics of decoherence processes and their underlying bipartite and multipartite interactions (collisions).

The basis for this diagnostics is the Kofman–Kurizki (KK) universal formula [29, 30, 34]

$$R(t) = \int F_t(\omega) G(\omega) d\omega$$
$$\leftrightarrow \text{change } \underbrace{F_t(\omega)}_{\text{Filter}} \Rightarrow \text{infer } \underbrace{G(\omega)}_{\text{Coupling}-\text{spectrum}} \quad . \quad (1)$$

The diagnostic method consists in changing the filter function $F_t(\omega)$, e.g., by varying the control-field Rabi frequency, recording the resulting decoherence rate $R(t)$ and deducing $G(\omega)$ from equation (1). To this end, the system, e.g. a qubit, is initially taken to be in a superposition of its excited ($|\uparrow\rangle$) and ground ($|\downarrow\rangle$) energy states. This initial superposition state

$$|\psi(0)\rangle = \cos\Theta |\uparrow\rangle + e^{-i\phi} \sin\Theta |\downarrow\rangle, \quad (2)$$

is subject to bath-induced decoherence (pure dephasing). It then has, at time t, a mean coherence that decays in a fashion dependent on $R(t)$

$$\langle \sigma_x(t) \rangle = e^{-R(t)t} \langle \sigma_x(0) \rangle, \quad (3)$$

which is inferred from the probabilities of measuring the system in the symmetric or antisymmetric superpositions of energy states (figure 1)

$$p_\pm(t) = \frac{1 \pm e^{-R(t)t}}{2}. \quad (4)$$

We have demonstrated (in collaboration with Davidson's group) [86] the ability to infer the bath-coupling spectrum $G(\omega)$ via formula (1) by measurements performed on a large ensemble of cold atoms in an optical trap. A field with narrow spectral band was used to realize a filter function $F_t(\omega)$ that scanned the overlap integral in equation (1) upon varying the field strength (Rabi frequency). By measuring the decoherence rate $R(t)$ as a function of the filter value we could infer the bath-coupling spectrum in the weak-coupling limit. This demonstration has experimentally established that the Kofman–Kurizki (KK) universal formula (1) allows the design of dynamical control (continuous-wave or pulse sequence) that is optimally adapted to the measured coupling spectrum of the bath.

2.2. Maximized information on the bath by dynamical control

We have recently been studying the maximum information obtainable on unknown spectral parameters of a bath (environment) by controlled spin qubits that serve as its probes [87]. This information is important for maximizing the sensitivity of spin probes at nanoscales, serving as magnetometers, thermometers, sensors for imaging or monitoring chemical and biological processes [88–91].

By using tools of quantum estimation theory, we can find the precision of estimating key parameters of environmental noises (baths) that the spin (qubit) can probe. These include the probe-bath coupling strength g, the correlation time of generic bath spectra τ_c, as well as their dephasing time T_2. By optimizing the dynamical control on the probe under realistic constraints one may achieve the best accuracy of estimating these parameters by the least number of measurements possible.

To this end, we minimize the relative error of estimating a bath parameter x_B by means of the dependence of the decoherence rate of a qubit-probe $R(t) \equiv R(x_B, t)$ on $G(\omega) \equiv G(x_B, \omega)$, as described by equations (1)–(4) (figure 1). This error obeys the bound

$$\epsilon(x_B, t) = \frac{\delta x_B}{x_B} \geqslant \frac{1}{x_B \sqrt{N_m \mathcal{F}_Q(x_B, t)}}. \quad (5)$$

Here we have introduced the number of measurements, N_m, and the quantum Fisher information (QFI) [92–95] for the qubit probe that is subject to dephasing as well as dynamical control

$$\mathcal{F}_Q(x_B, t) = \sin^2(2\Theta) \frac{e^{-2R(x_B, t)t}}{1 - e^{-2R(x_B, t)t}} \left(\frac{\partial R(x_B, t)t}{\partial x_B} \right)^2, \quad (6)$$

where Θ is as in equation (2). In general, we can minimize the relative error per measurement by maximizing QFI:

$$\mathcal{F}_Q(x_B, t_{opt}) = \max_t \mathcal{F}_Q(x_B, t) \quad (7)$$

which amounts to preparing the optimal initial state (2) with $\Theta = \frac{\pi}{4}$, measuring the qubit at the optimal time and efficiently controlling the quantum probe.

To demonstrate the potential of this approach, we may estimate, for example, the correlation time τ_c, a key parameter of Ornstein–Uhlenbeck processes characterized by Lorenztian bath spectra,

$$G(x_B, \omega) = \frac{g^2 \tau_c}{\pi \left(1 + \omega^2 \tau_c^2 \right)}, \quad (8)$$

assuming that the system–bath coupling strength g is known.

Dynamical control of the qubit probe can drastically improve the estimation of τ_c: as shown in figure 2, sequences of equidistant π-pulses (phase-flips), known as Carr–Purcell–Meiboom–Gill (CPMG) sequences [96–99], give rise to a minimal error estimation that obeys $\varepsilon_{CPMG}(\tau_c, t_{opt}) \simeq \frac{2.5}{\sqrt{N_m}}$, while under free evolution the error grows with $g\tau_c$, $\varepsilon_{free}(\tau_c, t_{opt}) \propto \frac{g\tau_c}{\sqrt{N_m}}$, and is therefore much larger for $g\tau_c \gg 1$, i.e. for distinctly non-Markovian bath spectra.
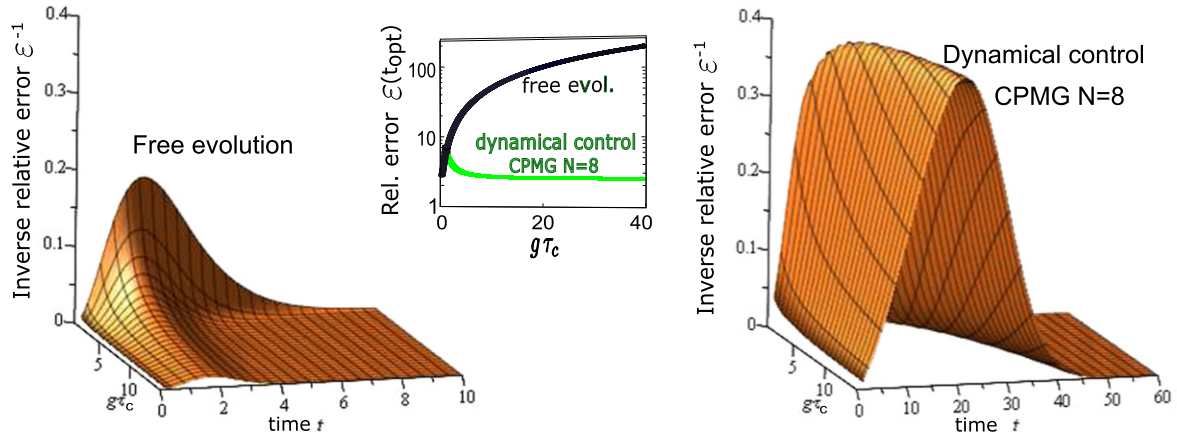
Figure 2. Estimation accuracy of the spectral width τ_c^{-1} of an Lorentzian bath with a quantum probe freely evolving (left) and dynamically controlled with a CPMG sequence of $N = 8$ π-pulses (right). The minimal error per measurement $\varepsilon\,(\tau_c,\,t_{\text{opt}})$ is much smaller for a qubit probe under optimal dynamical control than under free evolution (middle).

2.3. Bath-mediated transfer of quantum information

The ability to transfer an unknown quantum state between nodes where the quantum information (QI) can be reliably stored and / or processed is at the heart of QI processing and communication schemes. Since practically any medium connecting distant nodes corrupts the QI [100–102], one commonly resorts to probabilistic quantum repeaters [103], effected by conditional measurements [104]: only the desired outcomes are kept while the undesired outcomes are discarded. Such protocols [103] are severely constrained by high qubit-overhead and long average duration of successful QI transfer. It is clearly desirable to resort to deterministic protocols whenever possible. Here we advocate the possibility of such protocols, whose high success rate relies on dynamical control that is optimally adapted to the medium [79–81].

The idea is to write the full Hamiltonian as

$$H = H_{\text{S}} + H_{\text{B}} + H_{\text{SB}}. \tag{9}$$

Here the system S consists of the two spins that constitute the nodes between which the QI is transferred and a mode (channel) of the medium that couples these spins, labeled by $k = z$, all other modes being treated as a thermal bath B to which S is coupled.

The transfer fidelity over time T is again governed by the KK universal formula [34, 79]

$$F(T) \approx 1 - \int_{-\infty}^{\infty} \mathrm{d}\omega F_T(\omega) G(\omega). \tag{10}$$

We need not know the detailed spectral distribution of the S $-$B coupling $G(\omega)$, only its width $\frac{1}{\tau_c}$ and crude mode spacing, which can be estimated by the methods of sections 2.1–2.2. Such estimation should suffice for designing the optimal tradeoff of the fidelity F versus time transfer T by appropriate temporal modulation of the coupling. Strikingly, one may analytically prove [79], upon parameterizing the modulation

$$\alpha(t) = \alpha_0 \sin^p\left(\frac{\pi t}{T}\right) \quad p = 0, 1, 2 \quad |\alpha_0| \leqslant 1 \tag{11}$$

that the best tradeoff is usually achievable for $p = 2$, because it yields a filter function without spectral tails (these vanish abruptly at a controllable frequency). This chopping-off of the tails may reduce by several orders of magnitude the transfer infidelity (error) as well as the time required for transfer (figure 3)!

This control method, which is universally applicable to media consisting of interacting fermions (spin-$\frac{1}{2}$ particles) and bosons alike, may also be used to maximize the storage time of QI inside a bath memory embodied by an inhomogeneously broadened and thermally fluctuating spin ensemble [81]. Thus, the coupling between quantum systems via the bath is required for effecting QI transfer or storage, and system–bath interaction control may serve as a tool for optimizing these processes, on the basis of minimal knowledge concerning the bath. This method is another application of our universal procedure for fidelity optimization of the task at hand and the ability to prioritize the use of resources for implementing it in any given bath.

This method may be beneficial for the optimization of operating hybrid processors of quantum information comprised of different modules [77, 78, 105]: superconducting qubits coupled via a microwave resonator to ensembles of ultra-cold atoms or NV-center spins. Hybrid processors may profit from the advantages and make up for the shortcomings of the individual modules [105]. Specifically, the superconducting qubits are fast but vulnerable to decoherence. The outcome of their operations should be controllably transferred to collective 'quiet' (decoherence-resilient) states of the atoms that are much better suited for long-term shelving (storage) of this quantum information (QI). The overall fidelity of the processor can be improved by dynamical control that optimizes this QI transfer from the noisy to the quiet (storage) module. Remarkably, for a given energy of the transfer pulse, the shortest pulse is by no means optimal [80]!
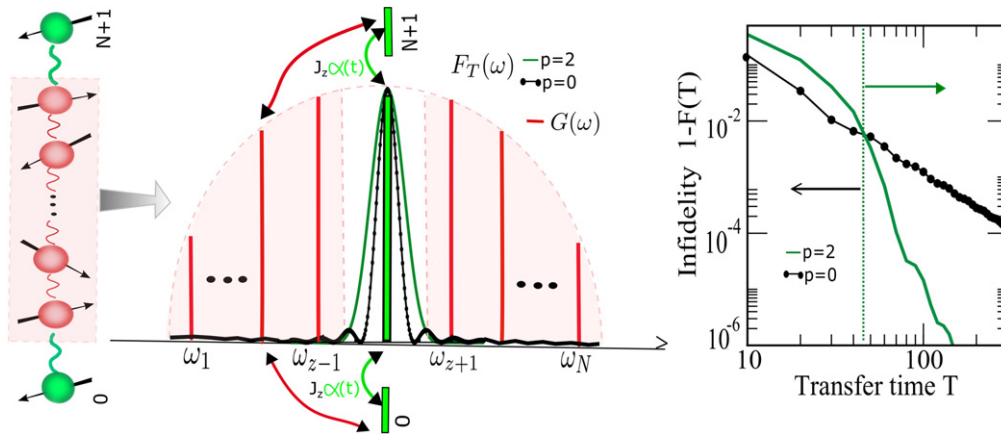
Figure 3. (Left) Schematic view of quantum information transfer through a fluctuating quantum spin-channel with random coupling *J*. The transfer over time *T* is optimized by an appropriate modulation $\alpha(t), |\alpha(t)| \leqslant 1$, of the boundary qubit-couplings to their nearest-neighbors. (Middle) schematic view of the coupling spectrum $G(\omega)$ between the 'system' (comprised of the two boundary qubits 0 and $N+1$ and the spin-chain mode that couples them) and all other modes of the spin chain viewed as a bath (red) and the filter $F_T(\omega)$ corresponding to the optimal chosen modulation shape $\alpha(t) \propto \sin^2\left(\frac{\pi t}{T}\right)$ (green) with chopped off tails, as compared to the (free evolution) filter (black), which has extended tails and therefore much larger overlap with $G(\omega)$. (Right) the chopping-off of the tails in the (green) filter may reduce by several orders of magnitude the transfer infidelity (error) as well as the time required for transfer.

A related method can significantly improve the performance of quantum memories based on spectrally inhomogeneous spin ensembles [81]. This method preselects an optimal portion of the ensemble by appropriate microwave pulse designs.

3. Bath-induced entanglement in open systems

Environment effects generally hamper or completely destroy the 'quantumness' of any complex device. Particularly fragile against environment effects is quantum entanglement (QE) in multipartite systems. This fragility may disable quantum information processing and other forthcoming quantum technologies [2–8, 105]: interferometry, metrology and lithography. Commonly, the fragility of QE rapidly mounts with the number of entangled particles and the temperature of the environment (thermal 'bath'). This QE fragility has been the standard resolution of the Schrödinger-cat paradox [14, 106]: the environment has been assumed to preclude macrosystem entanglement. But is it inevitable that Schrödinger cats die of decoherence (as commonly believed [13, 14])? Or, conversely, can a cat be both dead and alive in a thermal bath?

We shed light on these fundamental issues within the simple model of N spin-$\frac{1}{2}$ non-interacting particles that identically couple to a thermal oscillator-bath via the z-component of their Pauli operators. A single spin in such a model undergoes bath-induced pure dephasing [13, 14, 107]. Yet, strikingly [108, 109], an initial product state of *N* z-polarized spins can spontaneously evolve via such coupling to the bath, into a Schrödinger-cat state, also known as a macroscopic quantum superposition (MQS) or GHZ state [106],
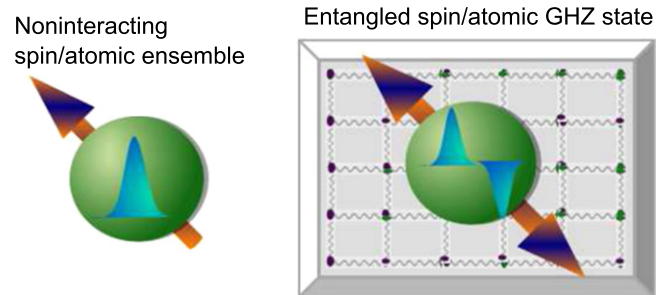

Figure 4. Schematic view of a product-state spin-polarized ensemble (left) that spontaneously evolves in the bath into an entangled MQS or GHZ (Schrödinger-cat) state at a particular time, as a result of bath-induced entanglement.

nearly deterministically (figure 4)

$$|\Uparrow\rangle \longrightarrow p\underbrace{\left(\frac{|\Uparrow\rangle + e^{i\frac{\pi}{2}}|\Downarrow\rangle}{\sqrt{2}}\right)\left(\frac{\langle\Uparrow| + e^{-i\frac{\pi}{2}}\langle\Downarrow|}{\sqrt{2}}\right)}_{\text{GHZ}}$$
$$+ (1-p)\rho_S, \, p \simeq 1 \qquad (12)$$

with $|\Uparrow\rangle = |\uparrow \uparrow ..\uparrow\rangle$, $|\Downarrow\rangle = |\downarrow \downarrow ..\downarrow\rangle$ and with only a small probability $1 - p$ of evolving into an incoherent state of the N spins.

This dynamics of the collective spin along z, $L_z = \sum_j \sigma_{zj}$, is driven by the Hamiltonian

$$H = \omega_0 L_z + \sum_k \omega_k b_k^\dagger b_k + \underbrace{L_z \sum_k \eta_k \left(b_k + b_k^\dagger\right)}_{H_I = L_z B: \text{ collective coupling to bath}} \qquad (13)$$

where $\omega_0 L_z$ stands for the collective energy (without the bath), b_k and $b_k^\dagger$, respectively, annihilate and create bath quanta in modes labeled by k, with frequencies ω_k and their coupling constants to L_z are denoted by η_k. The evolution of the combined system-bath state is *exactly soluble* by means of
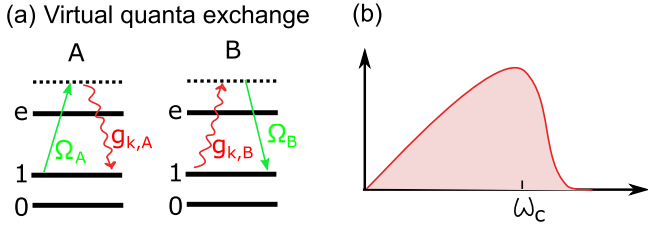
(a) Virtual quanta exchange   (b)

Figure 5. (a) Schematic view of bath-induced virtual quanta (wiggly arrows) exchanged between atoms A and B, in the presence of off-resonant fields (solid arrows). The net result is a collective interatomic energy (Lamb) shift. (b) An Ohmic bath spectrum allows for a collective Lamb shift associated with the integral over all bath frequencies ω, from 0 to ω_c, and thus dominates over the decoherence rate associated with the bath at $\omega \simeq 0$.

the unitary evolution operator [108, 109]

$$
U(t) = \exp\left(-\mathrm{i} \left(\omega_0 t L_z + \underbrace{f(t)L_z^2}_{\text{collective Lamb shift}} \right. \right.
$$
$$
\left. \left. + L_z t \sum_k \left(\alpha_k b_k + \alpha_k^* b_k^\dagger \right) \right) \right) \quad (14)
$$

Here the bath-induced nonlinear term is a collective Lamb shift (whose time-dependence is described by the bath-dependent function $f(t)$). This term does not affect the bath and only entangles the spins. The last term (wherein L_z is coupled to a linear combination of b_k ($b_k^\dagger$) with amplitudes α_k) gives rise to system–bath entanglement which, upon tracing out the bath, decoheres the spin-system state.

Clearly, the ability to entangle the spins via the bath-induced quadratic L_z^2 Lamb shift requires the suppression of the decoherence-inducing term (linear in L_z) in equation (14). This suppression is achievable by control, consisting of periodic phase flips that tend to average out the linear (odd-symmetry) term but leave intact the quadratic (even-symmetry) Lamb-shift term.

Further insight into the competing effects of bath-induced entanglement and decoherence can be obtained from a detailed consideration of a realistic model: two-atom dispersive coupling to a common cavity bath (figure 5(a)), described by the interaction Hamiltonian

$$
H_I = \sum_{j=\mathrm{A,B}} \sigma_{z,j} \mathrm{B}_j
$$
$$
= \sum_{j=\mathrm{A,B}} \sum_k \frac{\Omega_j g_{k,j}}{\Delta_j} \left| 1_j \right\rangle \left\langle 1_j \right| \left(b_k + b_k^\dagger \right) \quad (15)
$$

Here the energy shift of state $|1\rangle$ in atom j is caused by the combined effect of an off-resonant classical field (with Rabi frequency Ω_j and detuning Δ_j) and the quantized cavity field (with coupling strength $g_{k,j}$) (figure 5(a)). The cross-coupling of atoms $j = $ A, B via virtual quanta exchange in the cavity is the source of their collective Lamb shift. This cross-coupling is chosen not to depend on the interatomic distance under the assumption of identical couplings of both atoms to all cavity

modes:

$$
\eta_k = \frac{\Omega_j g_{k,j}}{\Delta_j} \quad (16)
$$

which is the case for atoms located at symmetric positions in the cavity. Then the foregoing analysis yields the real-quanta exchange rate between the atoms that causes decoherence

$$
\Gamma_{\mathrm{A(B)}} = 2\pi G_T(\omega = 0) \quad (17)
$$

where the coupling spectrum of the cavity-bath at temperature T is sampled at $\omega = 0$. This decoherence rate competes against the collective Lamb shift

$$
f_{\mathrm{AB}} = P \int d\omega \frac{G(\omega)}{\omega}. \quad (18)
$$

This two-atom Lamb shift is given by the principal-value part of the integral over the entire coupling spectrum, which, remarkably, is taken to be at zero temperature, $T = 0$, regardless of the actual bath temperature.

The desired dominance of the collective Lamb shift due to virtual quanta exchange over decoherence due to real quanta exchange, e.g., in an Ohmic bath, holds if

$$
f_{\mathrm{AB}} \gg \Gamma_{\mathrm{A(B)}} \text{ if } \omega_c \gg G_T(0). \quad (19)
$$

Namely, the upper cutoff frequency far exceeds the zero-frequency coupling rate, which is typically the case (figure 5(b)).

We thus arrive at the following paradigms: (i) QE in large multipartite systems may naturally (spontaneously) arise (albeit over limited time) when the system is embedded in commonly encountered thermal environments (baths). This QE may yield the spontaneous formation of Schrödinger-cat states (MQS). (ii) QE control may actually take advantage of the coupling to the environment rather than try to eliminate it, i.e., it should enhance the 'helpful' coupling, leading to virtual quanta exchange, and suppress the 'harmful' exchange of real quanta via the bath.

Such natural, yet unitary, evolution within thermal baths of the system to a highly-nonclassical MQS state is a universal effect which we dub bath-induced entanglement (BIE). Whereas, as a rule, the interaction of quantum system with a thermal bath gives rise to decoherence, BIE arises from nonresonant (virtual) interactions between particles via the bath: nonlinear frequency pulling. This is a generalization of effects that have previously been studied for multi-ion coupling to single-mode phonons [110].

A complementary (orthogonal) approach taken by other groups is to realize certain entangled states by engineering the incoherent (nonunitary) dissipation of quantum systems into a Markovian (spectrally flat) bath [111, 112]. By contrast, the coherent, bath-induced evolution discussed above crucially depends on having a non-flat bath spectrum.

Large ensembles of two-level atoms as considered above may be isomorphic to spin systems with large-spin eigenstates. The interaction of such ensembles with a common light field may lead to their entanglement [113]. Here, instead, we rely on the spectra of commonly encountered baths to drive
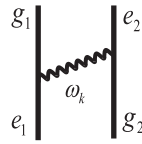
Figure 6. Photon-induced interaction between identical two-level atoms. Atom 1, initially in its upper state $|e_1\rangle$, emits a quantum at mode k and corresponding frequency ω_k while making a transition to its lower state $|g_1\rangle$. Atom 2, initially in its lower state, becomes excited upon absorbing the quantum. When the exchanged photon is real, i.e. for $\omega_k = \omega_a$ where ω_a is the frequency of the atomic transition, the interaction gives rise to dissipative, and hence probabilistic, cooperative-emission. The summation over all other virtual-photon-mediated processes, i.e. over all transition amplitudes for which $\omega_k \neq \omega_a$, yields the quantum-mechanically coherent and hence deterministic exchange process of resonant dipole–dipole interaction (RDDI).

Figure 7. Long-range RDDI in a fiber-grating. (a) Atoms (black dots) coupled to a fiber with a modulated refractive index (alternating blue and black colors) and a grating period of length Λ. (b) Illustration of the dispersion relation of the fiber-grating $\omega(k)$, k being the photon-mode wavenumber on the fiber axis: a gap at frequency ω and $k = \pi/\Lambda$ is opened up, with the upper bandedge at the upper cutoff frequency ω_{co}. (c) The density of longitudinal photon modes $\partial k/\partial \omega$ (inverse of group velocity v_g) vanishes in the gap and diverges at the bandedge ω_{co}. (d) RDDI mediated by the photon modes from (c): the excited-state population of atom 1 is plotted using a non-perturbative theory that goes beyond that of equation (21) [68]. This illustration is plotted for the D1 transition in Rb87 atoms and for an inter-atomic distance of $z \approx 16\mu$m (see [68] for more details). The population, initially unity, slightly decreases to 0.9663 and then oscillates periodically between 0.9663 and 0, similarly to the prediction of equation (21). This supports a long-distance entanglement generation with concurrence $C \approx 0.9663$ between the atoms at a distance of roughly 20 atomic resonant wavelengths, following an interaction duration of about $t \sim 1.8$ ns [68].

the spin ensemble into an entangled state, via effectively nonlinear dynamics.

At the same time, we must be concerned with the protection of such bath-induced entangled states from the disentangling effects of other baths that constitute their environment. Such protection presents a challenge: how to optimally control multiqubit entangled states? Our ability to face this challenge relies on our universal approach to multipartite decoherence control [43–45, 74–76] (see above).

4. Long-range bath-induced dispersive interactions

As argued above, the key to BIE is virtual quanta exchange via the bath. The BIE processes considered in section 3 were restricted to identical coupling of all the atoms to the bath modes, and hence their collective Lamb shift is distance-independent. However, in general this is not the case: the system–bath couplings in the interaction Hamiltonian depend on the positions of the individual atoms via the spatial mode functions of the bath modes. In free space the mode functions of the photonic bath are 3d plane waves, giving rise to real and virtual quanta exchange which both decay with interatomic separations r and correspond to Dicke-like cooperative emission/absorption and to cooperative Lamb shifts (i.e. resonant dipole–dipole interaction—RDDI), respectively [114, 115]. Whereas for interatomic separations r longer than the resonant atomic wavelength the real- and virtual-photon processes are comparable (scaling as $1/r$), in the near-field zone, i.e. for small r, the RDDI retains the familiar dipole-dipole scaling as $1/r^3$, and can greatly exceed cooperative decay. Therefore, only in the near-field zone can free-space RDDI lead to predominantly deterministic BIE. In contrast, RDDI-induced entanglement is never deterministic at separations beyond the emission wavelength, where incoherent absorption and emission render it probabilistic (figure 6).
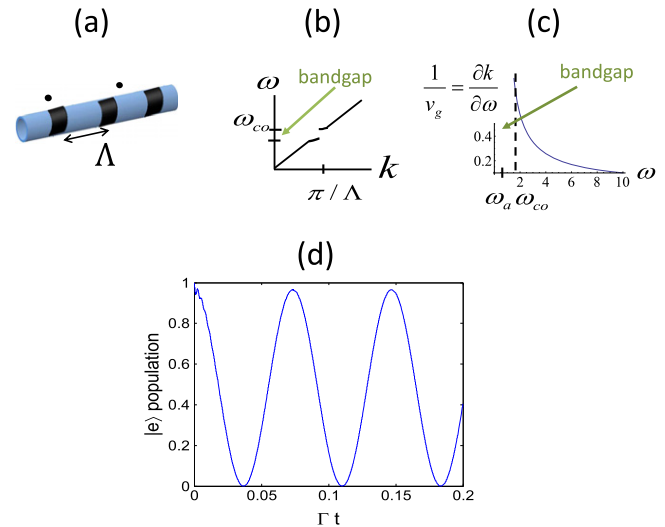
4.1. Long-range deterministic entanglement via RDDI

There is a remedy to this state of affairs that would render BIE via RDDI nearly deterministic in the far zone, i.e. for atoms separated by many wavelengths. This remedy is based on bath engineering: shaping photon modes at will by changing the geometry of the bath. The idea is to consider optical waveguides, such as a Bragg grating, where the group velocity of guided photonic modes vanishes at the cutoff (band-edge) frequency, giving rise to giant enhancement of the mode density [65, 68–70, 116] (figures 7(a)–(c)). Then, considering atomic resonance frequencies within the bandgap but very close to its bandedge (cutoff frequency), two consequences emerge. (1) The atoms do not exchange real (resonant) quanta (cooperative decay) along the waveguide due to the vanishing photon density of states at the atomic resonance, thus eliminating their probabilistic, dissipative, interaction. (2) The atoms do however, exchange virtual (nonresonant) quanta via RDDI, mediated by all allowed waveguide modes (see caption of figure 6). Furthermore, the resulting RDDI exhibits a strongly enhanced interaction rate (energy) Δ and effective
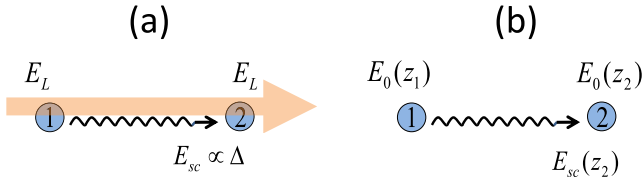
Figure 8. Dispersive forces between atoms. (a) Laser-induced forces: an off-resonant laser field E_L illuminates atoms 1 and 2. The scattered field between them, proportional to the RDDI strength Δ, establishes their interaction. (b) Vacuum-induced forces (van der Waals and Casimir): here the laser is replaced by the electric field of the vacuum fluctuations $E_0(z)$ (see text).

range ξ, scaling as

$$\Delta \propto \frac{\Gamma_{fs}}{\sqrt{1 - \omega_a/\omega_{co}}},$$

$$\xi \propto \frac{\lambda_a}{\sqrt{1 - \omega_a/\omega_{co}}}. \tag{20}$$

The above expressions reveal a RDDI whose strength Δ is much larger than the free-space spontaneous emission rate Γ_{fs}, and much longer-range than the atomic resonance wavelength λ_a, as the atomic resonance frequency ω_a approaches the cutoff (bandedge) frequency ω_{co}. Since spontaneous emission, being inhibited into the guided modes, remains at the free-space value whereas RDDI now has a giant value, we may describe the interatomic exchange of a photon by the effective Hamiltonian that affects two-atom entanglement nearly-deterministically, i.e., with high fidelity (figure 7(d),

$$H_{\text{eff}} = \hbar \Delta \sum_{\substack{i,j=1,2 \\ i \neq j}} \sigma_i^+ \sigma_j^- \tag{21}$$

where σ_i^+ (σ_j^-) are the excitation (deexcitation) Pauli operators of the respective atoms.

4.2. Long-range laser-induced forces

The same principle that allows for the establishment of coherent BIE via RDDI while suppressing the incoherent and dissipative process of emission, can be used to create long-range *conservative forces* between atoms. When atoms are illuminated by an off-resonant laser, their motion is affected by two processes in analogy to RDDI and spontaneous emission: an inter-atomic conservative force, and a diffusive motion due to the scattering, respectively. The direct relation to RDDI and spontaneous emission can be seen from the following picture (figure 8(a)): the off-resonant laser virtually excites the atoms, which, once excited, can either interact coherently via RDDI, leading to a distance-dependent cooperative energy shift and hence a force, or emit photons, leading to scattering [117].

For atoms coupled to a waveguide with a bandgap spectrum as in figure 7, and illuminated by an off-resonant laser, the resulting laser-induced force follows the same RDDI strength and range as in equation (20), while the
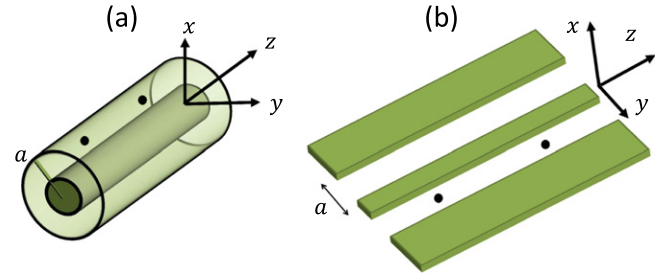

Figure 9. Atoms (black dots) coupled to a transmission-line (TL): a TL is typically comprised of two distinct conductors. (a) A coaxial TL comprised of two concentric conducting cylinders. (b) A coplanar waveguide may be seen as an open version of the coaxial line. It is comprised of a central conductor and two other grounded conductors (at a distance a from the center).

scattering and hence the diffusion, is suppressed. Therefore, the dynamics of the motion of atoms in such a system are predominantly affected by an extremely long-range conservative force. Such a configuration opens the door for the realization and control of many atoms coupled by long-range forces, that are expected to exhibit unique thermodynamic features, such as inequivalence of statistical ensembles and anomalously slow relaxation to equilibrium [62].

4.3. Long-range vacuum-induced forces

Even more dramatic, giant, enhancement is achievable via the control of the bath-geometry, for dipolar forces induced by the electromagnetic vacuum, namely, the Casimir and van der Waals (vdW) forces. The idea is to consider atoms coupled to an electric transmission line (TL), such as a coaxial cable or coplanar waveguide [61] (figure 9), which support the propagation of quasi-1d transverse electromagnetic (TEM) modes. Then, virtual excitations (photons) of these extended modes can mediate much stronger and longer-range Casimir and vdW forces than in free-space.

The unique feature of the fundamental TEM modes is their dispersion-free and diffraction-free 1d propagation, revealed by the k-dependence of their frequency ω_k and spatial mode function $u_k(\mathbf{r})$,

$$\omega_k = |k|\,c, \qquad u_k(\mathbf{r}) = \frac{e^{ikz}}{\sqrt{A(x,y)L}}, \tag{22}$$

k being the wavenumber in the longitudinal waveguide direction z and A the mode area.

The contribution of the TEM modes to the Casimir and vdW potentials can be evaluated by fourth order perturbation theory that yields the energy shift of two atoms in their lowest (ground) states coupled to the vacuum of the modes in equation (22) [118]. An alternative approach consists in recalling the expression for the energy of an electric dipole, $U = -(1/2)\alpha E^2$, where α is the dipolar polarizability and E is the field at the position of the dipole [119, 120]. Considering the energy of, e.g., atom 2, the electric field at its position z_2 along the transmission line, is comprised of the ordinary vacuum fluctuations, $E_0(z_2)$, and those scattered by atom 1 and subsequently arriving at atom 2, $E_{sc}(z_2)$. To
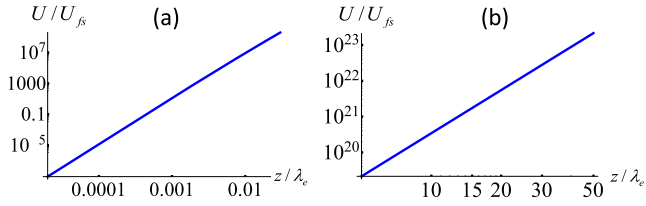
Figure 10. TEM-mediated vacuum energy U between a pair of atoms at a distance z, coupled to a TL with transverse dimension $a = 10^{-4}\lambda_e$, where λ_e is a characteristic dipole-transition wavelength (typical of coplanar-waveguide circuit-QED setups), compared to its free-space counterpart U_{fs}: (a) near-zone limit $z \ll \lambda_e$ (vdW regime); (b) far-zone limit $z \gg \lambda_e$ (Casimir-Polder regime).

lowest order in the scattering, this scattered field is found by the 1d propagation equation of the TEM modes, driven by the polarization at the location of atom 1, $E_0(z_1)$ (figure 8(b))

$$\left(\partial_z^2 + k^2\right)E_{sc,k}(z) = -\mu_0\omega_k^2\alpha_1(\omega_k)E_{0,k}(z_1)\delta(z-z_1)/A, \tag{23}$$

where k is the wavenumber of the field fluctuations. The solution of the above equation yields $E_{sc,k}(z_2)$ in terms of $\alpha_1(\omega_k)E_{0,k}(z_1)$. On the other hand, the interaction energy between the atoms 1 and 2, deduced from the dipolar energy U of atom 2, is related to the scattered-field and hence, to lowest order in the scattering, is given by,

$$U_{12} \propto -\sum_k \alpha_2(\omega_k)\left[E_{sc,k}(z_2)E_{0,k}(z_2) + \text{h.c.}\right]$$
$$\propto -\sum_k \alpha_2(\omega_k)\alpha_1(\omega_k)\left[E_{0,k}(z_1)E_{0,k}(z_2) + \text{h.c.}\right]. \tag{24}$$

Finally, treating the vacuum fluctuations $E_{0,k}(z)$ as a quantum field operator, we average equation (24) with respect to the vacuum state and obtain the vacuum interaction energy between the atoms, mediated by the dominant TEM mode of the transmission line.

This enhanced interaction energy may be analytically evaluated in the form of a hypergeometric function F of the interatomic distance $z = |z_1 - z_2|$ scaled to a typical dipolar-transition wavelength λ_e. In the near zone, i.e. for z much shorter than this wavelength, we obtain a modified vdW interaction as compared to free space [61]

$$F(z) \approx \pi + 16\pi\frac{z}{\lambda_e}\ln\left(\frac{z}{\lambda_e}\right), \tag{25}$$

that falls off very differently with z than the inverse 6th power, $U \propto 1/z^6$, that characterizes the interaction in free space. By contrast, for far-zone distances (well beyond λ_e), we find [61]

$$F(z) \approx \frac{1}{(2\pi)^3}\left(\frac{\lambda_e}{z}\right)^3, \tag{26}$$

as compared to the inverse 7th power falloff in free space, $U \propto 1/z^7$. The resulting enhancement can be enormous, as seen in figure 10.

An important outcome of the enhancement of Casimir forces in such a TL structure may be the onset of
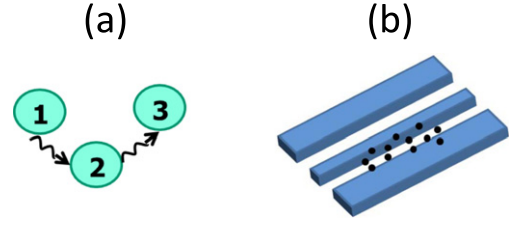

Figure 11. Nonadditivity of dispersive interactions. (a) The total energy of 3 atoms is given by the sum of their pairwise interactions $\sum_{ij=1}^{3} U_{ij}$ added to their 3-body interaction U_{123}, which is obtained by considering multiple scattering events involving all atoms. When U_{123} is negligible with respect to the pairwise summation part, the total energy is called *additive*. (b) A gas of atoms coupled to a transmission line, where nonadditive effects may be observed.
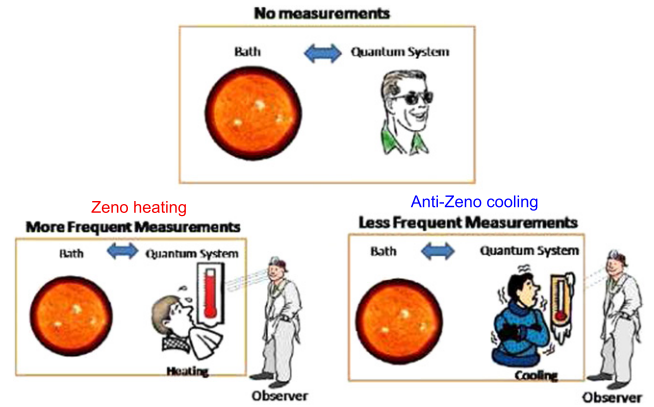

Figure 12. Cartoon of a quantum system whose thermal equilibrium with a bath (top) is changed towards progressive heating by highly frequent quantum non demolition (QND) measurements of its energy in the Zeno regime (bottom left) or towards progressive cooling by less frequent QND measurements in the anti-Zeno regime (bottom right) [48].

nonadditivity of atom–atom interactions [119–121] (figure 11(a)): already at rather low gas densities we expect that 3-body interactions U_{123} may become comparable to the strength of their usual pairwise counterpart U_{12}, because of the extension of the mediating photon modes in a TL over long distances. This means that the vacuum energy of a many-atom system may not be represented by the sum of its pairwise interactions U_{12}. More specifically, the ratio of 3-body to pairwise interaction energies in free space (3d) scales as [119, 120]

$$\left.\frac{U_{123}}{U_{12}}\right|_{3d} \propto \frac{\alpha}{z^3}. \tag{27}$$

Therefore, the inverse of the polarizability $1/\alpha$ sets the scale for a typical density $\sim 1/z^3$ where this ratio is large and nonadditivity is important. For the 1d TEM-mediated case, as in a TL, we find in the far-zone regime

$$\left.\frac{U_{123}}{U_{12}}\right|_{1d} \propto \frac{\alpha}{a^2 z}, \tag{28}$$

where $a \sim \sqrt{A}$ is transverse dimension of the TL. Then, for the typical case of $z \gg a$, where the TEM modes are
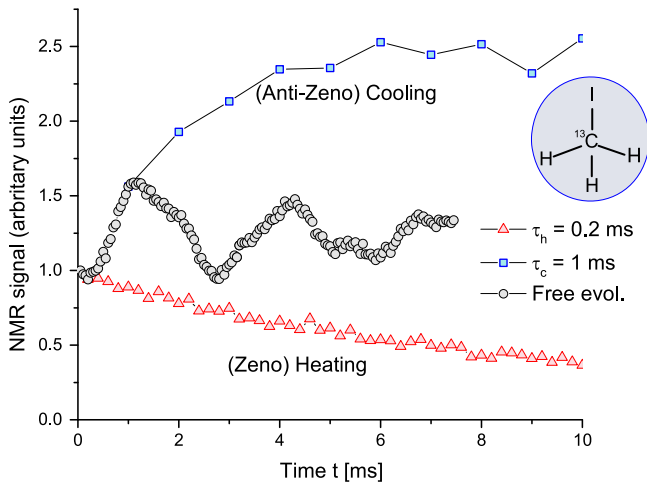
Figure 13. Experimental verification [107] of Zeno heating for QND polarization measurements (at intervals $\tau = 0.2$ ms) and anti-Zeno cooling (at intervals $\tau = 1$ ms), as in the cartoon above (figure 12). Experimental setup: quantum system embodied by the nuclear spin of a carbon atom C is in contact with a bath embodied by the nuclear spins of 3 protons. Their off-resonant frequency mismatch is changed by the measurements, causing polarization decrease (heating) or increase (cooling) of C depending on the interval τ.

dominant and 1d behavior prevails, nonaddivity is expected to become important at densities much lower than in free space. Among the possible consequences of this nonadditivity are drastic modifications of the effective dielectric response and the heat capacity of gases coupled to such structures (figure 11(b)).

5. Thermodynamic control via quantum Zeno and anti-Zeno effects

It is clearly desirable to cool down or purify a qubit at the fastest rate possible to make it suitable for tasks of quantum information processing. The standard, straightforward way of cooling a system such as a qubit is by equilibrating this system with a cold bath. But can one cool qubits faster than their equilibration time?

Another issue concerning cooling is that it often involves transitions between the qubit levels and other auxiliary levels. But what if such auxiliary levels are not available? We have shown that these two obstacles may be overcome by exerting highly frequent perturbations on a qubit, such as phase shift, or measurements [48] at intervals much shorter than the memory (correlation) time of the bath to which the qubit couples, and well within the equilibration times [49, 50]. In such a scenario, a non-Markovian treatment of the purification must be adopted [48–50, 107].

Specifically, we have experimentally and theoretically demonstrated (in collaboration with L Frydman's group) the possibility of purifying a qubit coupled to a spin bath, by means of repeated noise-induced dephasing that mimics the effect of a non-selective (unread) measurements. We have shown (figure 13) that the qubit may be cooled down to a predetermined temperature that may be much lower than that

of the bath by means of a suitable controlled dephasing rate, that conforms to the condition for the anti-Zeno effect (AZE). By contrast, a dephasing rate that corresponds to a quantum Zeno effect (QZE) leads to heating of the qubit [48–50, 107]. The qubit may exist in the state of predetermined purity to which it was driven by the measurements or dephasing as long as the entropy of the bath remains constant. A violation of this (Bonn) approximation will render the qubit as well as the bath fully mixed, i.e. will thermalize them to infinite temperature [49].

6. Heat-machine design by system-bath control: quantum thermodynamic bounds

6.1. Work-information tradeoff in the non-Markovian domain

Open-system manipulations must be optimized within thermodynamic bounds, concerning entropy, work and heat production. However, when these manipulations are faster than the bath memory time, so that the Markovian approximation does not hold, we must revisit and better understand these bounds. Part of the reason is that correlations between the system and the bath, which are ignored in standard thermodynamics, may play an important role on non-Markovian time scales. In particular, as discussed below, they may invalidate the bound set by Szilard, and more quantitatively by Landauer, on the tradeoff between information and work [122, 123].

System-bath correlation effects. All existing treatments of heat engines are based on the assumption that the working-medium (system) is *autonomous*: its evolution (described by a Lindblad-type master equation for the bath-averaged system-state $\rho_S(t)$) suffices for a thermodynamic analysis of an engine [124, 125] driven by Hamiltonian $H_S(t)$. Under this standard assumption, the following expression for the work, W, is expected to hold [124] for a closed cycle:

$$W = \oint tr\left\{\rho_S \dot{H}_S\right\} dt. \tag{29}$$

The convention is that the work W is negative if it is performed by the system on the external piston. According to Lindblad's H-theorem, or the Kelvin formulation of the second law, $W \geqslant 0$, i.e. the system cannot do work on the piston in a single-bath setup. Yet, strikingly, according to our results [126] if the cycle is faster than the bath memory time, the system may do net work on the piston! To resolve the paradox, we contend that, contrary to the standard assumption [124, 125], *it is wrong to assume that the system is autonomous in the quantum non-Markovian domain*: the correlations of the system with the bath are then crucial! Accordingly, we show that the second law is upheld if we allow for the energetic and entropic cost incurred upon *decorrelating the entangled system-bath state* that exists in thermal equilibrium by the measurement that triggers each cycle. The correct description must account for the *total* work during the cycle, evaluated by considering the total state ρ_{tot} and the Hamiltonian H_{tot} (of the system and the bath
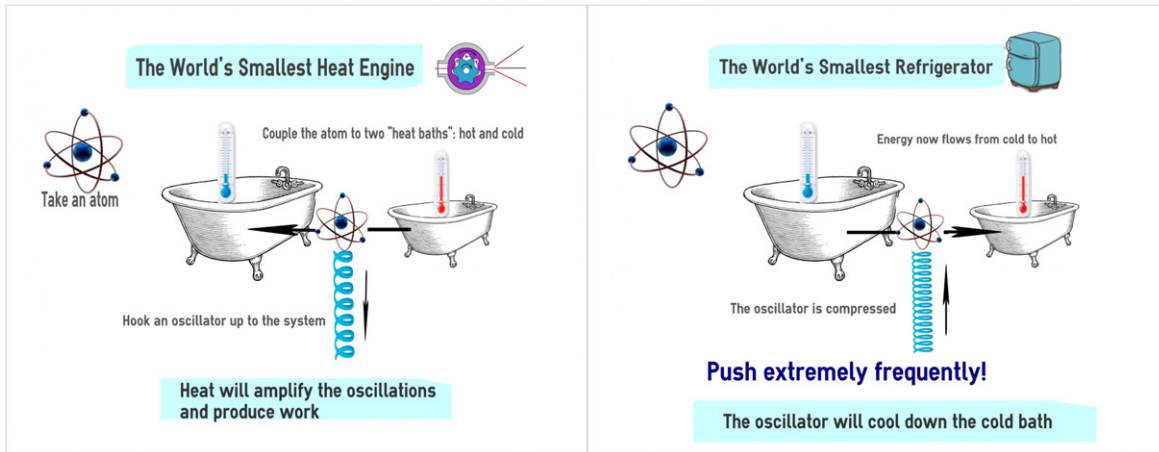
Figure 14. Cartoon of the 'world's simplest and smallest' universal heat machine acting as heat engine (left) or refrigerator (right). It is comprised of a qubit that constantly interacts with two baths at different temperatures. Concurrently, it is driven by an oscillator that off resonantly modulates (by periodic Stark shifts) the qubit resonance frequency. The modulation rate determines whether the qubit will act as a heat engines or refrigerator [71].

combined) [126]:

$$W_{\text{tot}} = \oint tr\left\{\rho_{\text{tot}}\dot{H}_{\text{tot}}\right\}dt. \qquad (30)$$

The non-negativity of the work $W_{\text{tot}} \geqslant 0$, under a closed-cycle (*unitary*) evolution of the Hamiltonian (H_{tot}), in keeping with the second law, is ensured by the inequality

$$W_{\text{tot}} = W + \Delta E > 0, \qquad (31)$$

where ΔE is the *measurement cost* of the system-bath decorrelation. Equation (30) may still allow the system to do net work during the cycle ($W < 0$), but it should compensate for this work by the energy cost ΔE of the system-bath state preparation. This cost comes about from changing the mean system-bath correlation energy from its negative equilibrium value [48–50] to zero (or positive value) after the preparation (e.g., via a brief measurement or phase-flip).

6.2. Minimal quantum heat machines

One of our main targets is the strive to realize the minimal and simplest thermal machines in the quantum domain. These may be conceived as (figure 14) quantized (harmonic-oscillator) 'piston' that couples to a single qubit acting as either a quantum heat engine (QHE) or quantum refrigerator (QR) on spectrally non-flat baths. Floquet analysis of periodically-driven open systems is used to treat their steady-state thermodynamics [71, 127]. This formalism aims to separate those distinctly non-Markovian (and non-rotating-wave) effects that may cause anomalous thermodynamic phenomena on short-time scales [48–50, 107] from steady-state thermodynamics.

The simplest variant to be used as a model for the minimal quantum thermal machine is a (frequency-modulated) qubit Hamiltonian

$$H(t) = \frac{1}{2}\omega(t)\sigma_z, \quad \omega\left(t + \frac{2\pi}{\Omega}\right) = \omega(t), \qquad (32)$$

where $\omega(t)$ is the periodic modulation about the qubit resonance ω_0 with frequency Ω. Its coupling to two heat baths is given by the interaction Hamiltonian

$$H_{\text{int}} = \sigma_x \otimes \left(B^h + B^c\right). \qquad (33)$$

where the bath operators (B^h, B^c) are respectively associated with hot (T_h) and cold (T_c) temperatures, as well as with *distinct spectra*. Using the period-averaged (coarse-grained) Floquet expansion, we can find the conditions for the coarse-grained density operator $\tilde{\rho}_S$ of the qubit to be a steady state of a Lindblad super-operator,

$$\mathcal{L}\tilde{\rho}_S = 0, \ \mathcal{L} = \sum_q \mathcal{L}_q^a, \qquad (34)$$

where $q = \pm 1, \pm 2, \ldots$ is the harmonic index, $a = c$, h is the bath index, and $\mathcal{L}_q^a \tilde{\rho}_S$ describes the steady-state with the qubit resonance ω_0 shifted by $q\Omega$, Ω being the periodic modulation frequency. This decomposition of the Liouvillian effectively replaces each bath by multiple q-harmonic 'sub-baths' with differently shifted coupling spectra. The merit of this equation is that it employs Lindblad (completely-positive) dynamics but still allows for non-flat bath spectra. This steady-state expansion can serve to evaluate the heat currents exchanged among the multiple harmonic 'sub-baths' via the qubit. These currents can be controlled and optimized by the modulation and the bath-spectrum engineering. Their signs will determine whether the machine functions as QHE or QR, *without the need* for traditional stroke cycles (Carnot, Curzon, Otto). We have studied these QHE and QR models in optomechanical [128] and spin-ensemble [129] setups.

We contend that such a periodically-modulated control qubit coupled to both baths is a *minimal model* for QHE and QR (figure 15). It is remarkable that such a simple model allows for both QHE and QR actions, by contrast to previous models that required 3-level [130, 131] or coupled-qubit [3, 4] configurations.

Under π-flip (periodic) modulation of the qubit there are only two dominant Floquet harmonics at $\omega = \omega_0 \pm \Omega$. If the
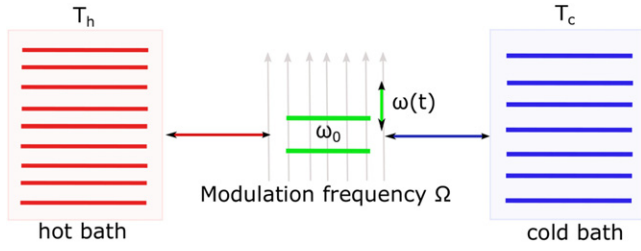
Figure 15. Components of the universal heat machine depicted in figure 14: (1) working fluid (qubit system); (2) two baths at different (hot and cold) temperatures, permanently coupled to the qubit (via weak coupling); (3) a piston (external field oscillator) that periodically modulates the qubit (level distance), i.e. $\omega(t)$ about the qubit frequency ω_0 and with modulation frequency (rate) Ω, and thereby extracts work (at expense of the hot bath) in the heat-engine regime, or provides work (in order to cool down the cold bath) in the refrigerator regime, depending on Ω [71].
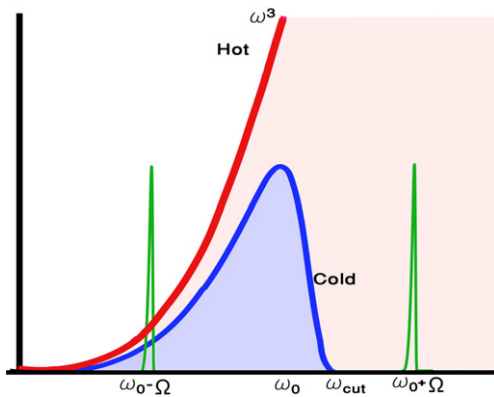

Figure 16. Separation of the hot and cold bath spectra required for the universal heat machine in figures 14–15. The hot-bath spectrum $G^h(\omega)$ (red) is that of black body radiation, rising with mode density as ω^3, whereas the cold bath spectrum $G^c(\omega)$ (blue, Lorentzian or Ohmic) extends up to ω_{cut}. The periodic modulation (π-flips) of the qubit creates two sidebands (green): the lower overlaps both bath spectra, but the upper only overlaps the hot-bath spectrum [71].

cold-bath coupling spectrum $G^c(\omega)$ has an upper cutoff, such that the hot-bath spectra $G^h(\omega = \omega_0 + \Omega)$ dominates at high energies, but $G^c(\omega = \omega_0 - \Omega)$ dominates at low frequencies (figure 16), then the heat flow from the cold to the hot bath (cold current) J_c is proportional to the product of the respective hot- and cold-bath spectra,

$$J_c \propto G^h(\omega_0 + \Omega)G^c(\omega_0 - \Omega). \tag{35}$$

Under this condition J_c is positive if

$$n_h(\omega_0 + \Omega) < n_c(\omega_0 - \Omega) \tag{36}$$

where n_h and n_c are the respective thermal bath occupancies. We then obtain QR action, namely, heat removal from the cold bath and its dumping into the hot bath. The opposite inequality sign implies work production. Thus we have a *single control parameter*, the modulation rate, Ω: for low rates we have an engine (QHE) and for high ones a heat pump (QR) (figure 17). However, neither the QHE nor the QR action will happen if the bath spectra are inappropriate, so that bath-spectrum engineering is crucial.
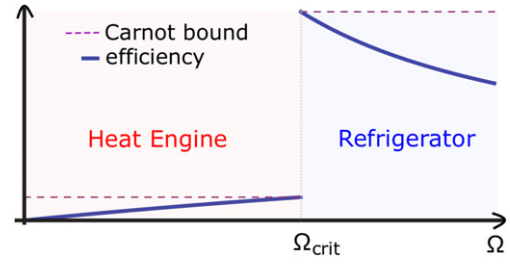

Figure 17. Performance of the universal heat machine depicted in figures 14–16 (under the assumption that the spectra of the two baths are non-overlaping (separated)). The efficiency is plotted as a function of the modulation rate Ω [71]. The efficiency in the heat engine regime rises with Ω up to the Carnot bound at $\Omega = \Omega_{crit}$. At higher Ω the machine switches over to the refrigerator regime with a coefficient of performance that decreases from the Carnot bound.

6.3. Third-law issues

The limits on cooling power and efficiency of this unconventional QR can serve to probe the validity of one of the formulations of the third law of thermodynamics by Nernst that prohibits the attainability of zero temperature in finite time. To this end, we explore the use of a *single driven qubit simultaneously* coupled to hot and cold spectrally non-flat baths. The possibility of cooling a bath down to arbitrarily low temperatures, i.e. *cooling rate scaling with temperature,* is thus a fundamental issue that reflects on the applicability of the third law. As a typical example we assume that the QR pumps heat into an infinite hot bath, and out of a cold bath whose *heat capacity is finite* $c_V < \infty$, resulting in $T_c = T_c(t)$. Strikingly, we may show that *arbitrarily low temperature* may be reached at *finite time* (non-exponentially fast) by the heat pump, for an appropriate (magnon) cold-bath spectrum thereby challenging the third law [73].

7. Conclusions and outlook

Progress in technologies such as quantum information processing (QIP) and quantum precision measurements (QPM) or metrology is currently restricted by our ability to either minimize the environment effects or actively suppress them by 'dynamical decoupling'. Based on our theoretical and experimental work, we advocate instead taking advantage of the environment (bath) as a resource for quantum technologies, provided that we optimize its beneficial effects, preferably by non-unitary open-system manipulations that are less restrictive and more robust than unitary operations.

To this end, we have identified the following generic tools:

- **Universal dynamical control** of open quantum systems, be it coherent or projective (nonunitary) that can be optimized (in terms of energy investment) for the desired operational task and bath spectrum at hand. Such optimized control may conform to one of two paradigms: the quantum Zeno effect (QZE) or the anti-Zeno effect (AZE), depending on the task (section 2). In particular,

we have introduced the use of dynamical control as a means of maximizing the quantum Fisher information (or estimation accuracy) regarding the bath spectrum (sections 2.1–2.2). We have also resorted to our universal dynamical control for optimizing the tradeoff between the fidelity and duration of quantum information transfer via noisy and random media which we model as baths (section 2.3).

- **Bath geometry control** by mode confinement to one dimension and spectral-cutoff design has been shown (section 4) to allow for drastic increase in the range and fidelity of bath-induced atom-atom entanglement (sections 3, and 4.1) and, even more dramatically, the giant enhancement of dispersion (Casimir) forces (section 4.3). These dispersive mechanisms rely on virtual-quanta exchange via the bath, which is enhanced by the engineered bath geometry, as opposed to dissipative (real-quanta) exchange, which is suppressed by the chosen bath geometry.

- **Bath-spectra engineering** has been shown to be a prerequisite for thermodynamic control: AZE employed for high-speed qubit cooling (section 5); the intriguing possibility of exceeding the Szilard–Landauer bound by taking advantage of system-bath correlations (section 6.1); the operation of simple (minimal) quantum heat machines based on a periodically-modulated qubit that can attain both high efficiency (near the Carnot bound) and power (section 6.2); as well as challenging Nernst's formulation of the third law for the cooling of a magnon bath towards the absolute zero (section 6.3).

We are confident that, however intriguing the above results are, they just barely 'scratch the surface' insofar as bath-assisted quantum processes are concerned. Inevitably, such processes are within the realm of quantum thermodynamics. In order to be able to benefit from the quantum control tools discussed above, we should revisit the foundations of thermodynamics and reformulate its key concepts and laws by (i) removing the system-bath partition; (ii) exploring coherence and entanglement effects on thermodynamic variables and (iii) substantiating such fundamental effects by studies of different realizations: NV-center spins coupled to a spin bath, spin-boson models and boson-boson models in optomechanics.

The corresponding conceptual goals of such future research are foreseen to be as follows:

a) Use bath engineering, i.e. control of its dimensionality, coupling spectrum and quantum state, as a key resource in an effort to push the thermodynamic limits of quantum device performance: (i) long-time non-Markovian behavior is expected for qubits near-resonant with an abrupt spectral cutoff of a quasi 1D bath previously studied by us [132]. Extensions of these effects to finite-temperature baths may be prerequisites to pushing thermodynamics into the hitherto unexplored strong-coupling regime where system-bath separability breaks down. This regime is expected to allow for (partial) reversibility of the entropy and work and thereby alter

quantum heat engine (QHE), quantum refrigerator (QR) and quantum memory device (QMD) performance. (ii) Novel methods of controlling system-bath coupling by measurements or phase flips at intervals that violate Markovianity, can be developed so as to steer the system-bath dynamics towards desired outcomes.

b) Reexamine the work-effciency Carnot limit derived within the system-bath separability (weak-coupling) paradigm: little is known about the strong-coupling regime in thermodynamics, and we may not rule out that it has surprises in store insofar as performance bounds of quantum heat machines are concerned [11], since the known definitions of heat currents and power output no longer apply in that regime.

c) Discover quantum-operations speed limits in the thermodynamic limit: the rates (speed) of quantum information storage and retrieval, cooling and heat engine cycles of quantum systems coupled to thermal baths have unknown thermodynamic bounds. To understand these bounds, we should extend our previous studies of the third law [73] by discovering the scaling of bath cooling-rate with temperature T as $T \to 0$.

To conclude, thermal baths are promising to be 'more friends than foes' for exploiting the quantumness of systems that couple to such baths, provided that appropriate dynamical control and bath engineering are implemented.

Acknowledgments

References

[1] Scully M O and Zubairy M S 1997 *Quantum Optics* (Cambridge: Cambridge University Press)

[2] Nielsen M A and Chuang I L 2000 *Quantum Computation and Quantum Information* (Cambridge: Cambridge University Press)

[3] Gisin N, Ribordy G, Tittel W and Zbinden H 2002 *Rev. Mod. Phys.* **74** 145–95

[4] Sergienko A V 2005 *Quantum Communications and Cryptography* (Boca Raton, FL: CRC)

[5] Giovannetti V, Lloyd S and Maccone L 2011 *Nat. Photonics* **5** 222–9

[6] Wolfgramm F, Vitelli C, Beduini F A, Godbout N and Mitchell M W 2013 *Nat. Photonics* **7** 28–32

[7] Schmidt P O, Rosenband T, Langer C, Itano W M, Bergquist J C and Wineland D J 2005 *Science* **309** 749–52

[8] Hempel C, Lanyon B P, Jurcevic P, Gerritsma R, Blatt R and Roos C F 2013 *Nat. Photonics* **7** 630–3

[9] Ockeloen C F, Schmied R, Riedel M F and Treutlein P 2013 *Phys. Rev. Lett.* **111** 143001

[10] Gemmer J, Michel M and Mahler G 2010 *Quantum Thermodynamics: Emergence of Thermodynamic Behavior Within Composite Quantum Systems* (*Lecture Notes in Physics* vol 657) (Berlin: Springer)

[11] Scully M O, Zubairy M S, Agarwal G S and Walther H 2003 *Science* **299** 862–4

[12] Scully M O, Chapin K R, Dorfman K E, Kim M B and Svidzinsky A 2011 *Proc. Natl Acad. Sci.* **108** 15097–100
[13] Breuer H P and Petruccione F 2002 *The Theory of Open Quantum Systems* (Oxford: Oxford University Press)
[14] Zurek W H 2003 *Rev. Mod. Phys.* **75** 715–75
[15] Viola L and Lloyd S 1998 *Phys. Rev.* A **58** 2733–44
[16] Agarwal G S, Scully M O and Walther H 2001 *Phys. Rev.* A **63** 044101
[17] Agarwal G S 2000 *Phys. Rev.* A **61** 013809
[18] Shiokawa K and Lidar D A 2004 *Phys. Rev.* A **69** 030302
[19] Vitali D and Tombesi P 2001 *Phys. Rev.* A **65** 012305
[20] Viola L and Knill E 2003 *Phys. Rev. Lett.* **90** 037901
[21] Khodjasteh K and Lidar D A 2005 *Phys. Rev. Lett.* **95** 180501
[22] Dicke R H 1954 *Phys. Rev.* **93** 99
[23] Prasad S and Glauber R J 2000 *Phys. Rev.* A **61** 063814
[24] Wiegner R, von Zanthier J and Agarwal G S 2011 *Phys. Rev.* A **84** 023805
[25] Scully M O, Fry E S, Ooi C R and Wódkiewicz K 2006 *Phys. Rev. Lett.* **96** 010501
[26] Scully M O and Svidzinsky A A 2009 *Science* **325** 1510–1
[27] Mazets I E and Kurizki G 2007 *J. Phys. B: Atom. Mol. Phys.* **40** 105
[28] Misra B and Sudarshan E C G 1977 *J. Math. Phys.* **18** 756–63
[29] Kofman A G and Kurizki G 2000 *Nature* (*London*) **405** 546–50
[30] Kofman A G and Kurizki G 2001 *Phys. Rev. Lett.* **87** 270405
[31] Facchi P, Nakazato H and Pascazio S 2001 *Phys. Rev. Lett.* **86** 2699
[32] Lane A M 1983 *Phys. Lett.* A **99** 359–60
[33] Fischer M C, Gutierrez-Medina B and Raizen M G 2001 *Phys. Rev. Lett.* **87** 040402
[34] Kofman A G and Kurizki G 2004 *Phys. Rev. Lett.* **93** 130406
[35] Kofman A G, Kurizki G and Opatrný T 2001 *Phys. Rev.* A **63** 042108
[36] Kofman A G and Kurizki G 1996 *Phys. Rev.* A **54** 3750–3
[37] Pellegrin S and Kurizki G 2004 *Phys. Rev.* A **71** 032328
[38] Gordon G, Kurizki G and Lidar D A 2008 *Phys. Rev. Lett.* **101** 010403
[39] Kofman A G and Kurizki G 2005 *IEEE Trans Nanotechnol.* **4** 116
[40] Gordon G, Kurizki G and Kofman A G 2006 *Opt. Comm.* **264** 398
[41] Barone A, Kurizki G and Kofman A G 2004 *Phys. Rev. Lett.* **92** 200403
[42] Gordon G, Kurizki G and Kofman A G 2005 *J. Opt.* B **7** 283
[43] Gordon G and Kurizki G 2006 *Phys. Rev. Lett.* **97** 110503
[44] Gordon G, Erez N and Kurizki G 2007 *J. Phys. B: At. Mol. Opt. Phys.* **40** 75–93
[45] Gordon G and Kurizki G 2007 *Phys. Rev.* A **76** 042310
[46] Facchi P and Pascazio S 2002 *Phys. Rev. Lett.* **89** 080401
[47] Brion E, Akulin V M, Comparat D, Dumer I, Harel G, Kèbaili N, Kurizki G, Mazets I and Pillet P 2005 *Phys. Rev.* A **71** 052311
[48] Erez N, Gordon G, Nest M and Kurizki G 2008 *Nature* **452** 724
[49] Gordon G, Rao D D B and Kurizki G 2010 *New J. Phys.* **12** 053033
[50] Gordon G, Bensky G, Gelbwaser-Klimovsky D, Rao D, Erez N and Kurizki G 2009 *New J. Phys.* **11** 123025
[51] Kurizki G, Kofman A G and Yudson V 1996 *Phys. Rev.* A **53** R35
[52] Sherman B and Kurizki G 1992 *Phys. Rev.* A **45** 7674
[53] Kozhekin A, Kurizki G and Sherman B 1996 *Phys. Rev.* A **54** 3535–8
[54] Sherman B, Kurizki G and Kadyshevitch A 1992 *Phys. Rev. Lett.* **69** 1927–30
[55] Kurizki G, Sherman B and Kadyshevitch A 1993 *JOSA* B **10** 346–52
[56] Li J *et al* 2008 *Opt. Express* **16** 12899–904

[57] Petrosyan D and Kurizki G 2002 *Phys. Rev. Lett.* **89** 207902
[58] Kurizki G and Haus J W 1994 *J. Mod. Opt.* **41** 171–2
[59] Friedler I, Kurizki G and Petrosyan D 2005 *Phys. Rev.* A **71** 023803
[60] Kurizki G 1990 *Phys. Rev.* A **42** 2915–24
[61] Shahmoon E, Mazets I and Kurizki G 2014 *Proc. Natl Acad. Sci.* **111** 10485–90
[62] Shahmoon E, Mazets I and Kurizki G 2014 *Opt. Lett.* **39** 3674–7
[63] Friedler I, Petrosyan D, Fleischhauer M and Kurizki G 2005 *Phys. Rev.* A **72** 043803
[64] Petrosyan D and Kurizki G 2001 *Phys. Rev.* A **64** 023810
[65] Shahmoon E, Kurizki G, Fleischhauer M and Petrosyan D 2011 *Phys. Rev.* A **83** 033806
[66] Friedler I, Kurizki G and Petrosyan D 2004 *EPL* **68** 625
[67] Mandilara A, Akulin V M, Kolar M and Kurizki G 2007 *Phys. Rev.* A **75** 022327
[68] Shahmoon E and Kurizki G 2013 *Phys. Rev.* A **87** 033831
[69] Shahmoon E and Kurizki G 2013 *Phys. Rev.* A **87** 013841
[70] Shahmoon E and Kurizki G 2013 *Phys. Rev.* A **87** 062105
[71] Gelbwaser-Klimovsky D, Alicki R and Kurizki G 2013 *Phys. Rev.* E **87** 012140
[72] Gelbwaser-Klimovsky D, Alicki R and Kurizki G 2013 *Europhys. Lett.* **103** 60005
[73] Kolář M, Gelbwaser-Klimovsky D, Alicki R and Kurizki G 2012 *Phys. Rev. Lett.* **109** 090601
[74] Gordon G and Kurizki G 2011 *Phys. Rev.* A **83** 032321
[75] Clausen J, Bensky G and Kurizki G 2010 *Phys. Rev. Lett.* **104** 040401
[76] Clausen J, Bensky G and Kurizki G 2012 *Phys. Rev.* A **85** 052105
[77] Petrosyan D, Bensky G, Kurizki G, Mazets I, Majer J and Schmiedmayer J 2009 *Phys. Rev.* A **79** 040304
[78] Bensky G, Amsüss R, Majer J, Petrosyan D, Schmiedmayer J and Kurizki G 2011 *Quant. Inf. Proc* **10** 1037–60
[79] Zwick A, Álvarez G A, Bensky G and Kurizki G 2014 *New J. Phys.* **16** 065021
[80] Escher B M, Bensky G, Clausen J and Kurizki G 2011 *J. Phys. B: At. Mol. Opt. Phys.* **44** 154015
[81] Bensky G, Petrosyan D, Majer J, Schmiedmayer J and Kurizki G 2012 *Phys. Rev.* A **86** 012310
[82] Bar-Gill N, Gross C, Mazets I, Oberthaler M and Kurizki G 2011 *Phys. Rev. Lett.* **106** 120404
[83] Bhaktavatsala Rao D D, Bar-Gill N and Kurizki G 2011 *Phys. Rev. Lett.* **106** 010404
[84] Bhaktavatsala Rao D D and Kurizki G 2011 *Phys. Rev.* A **83** 032105
[85] Souza A M, Álvarez G A and Suter D 2012 Phil. Trans. R. Soc. A **370** 4748–69
[86] Almog I, Sagi Y, Gordon G, Bensky G, Kurizki G and Davidson N 2011 *J. Phys. B: At. Mol. Opt. Phys.* **44** 154006
[87] Zwick A, Alvarez G A and Kurizki G 2015 preprint arXiv:1507.03281
[88] Neumann P *et al* 2013 *Nano Lett.* **13** 2738–42
[89] McGuinness L *et al* 2011 *Nat. Nanotechnol.* **6** 358–63
[90] Smith P E S, Bensky G, Álvarez G A, Kurizki G and Frydman L 2012 *Proc. Natl Acad. Sci.* **109** 5958–61
[91] Álvarez G A, Shemesh N and Frydman L 2013 *Phys. Rev. Lett.* **111** 080404
[92] Braunstein S and Caves C 1994 *Phys. Rev. Lett.* **72** 3439–43
[93] Paris M G A 2009 *Int. J. Quantum Inf.* **07** 125–37
[94] Benedetti C and Paris M G A 2014 *Phys. Lett.* A **378** 2495
[95] Escher B M, de Matos Filho R L and Davidovich L 2011 *Nat. Phys.* **7** 406–11
[96] Carr H Y and Purcell E M 1954 *Phys. Rev.* **94** 630
[97] Meiboom S and Gill D 1958 *Rev. Sci. Instrum.* **29** 688

[98] Abragam A 1961 *Principles of Nuclear Magnetism* (London: Oxford University Press)

[99] Slichter C P 1990 *Principles of Magnetic Resonance* (Berlin: Springer)

[100] Zwick A, Álvarez G A, Stolze J and Osenda O 2011 *Phys. Rev.* A **84** 22311

[101] Zwick A, Álvarez G A, Stolze J and Osenda O 2012 *Phys. Rev.* A **85** 012318

[102] Stolze J, Álvarez G A, Osenda O and Zwick A 2014 Robustness of spin-chain state-transfer schemes *Quantum State Transfer and Quantum Network Engineering* (*Quantum Science and Technology Series*) ed G M Nikolopoulos and I Jex (Berlin: Springer)

[103] Duan L M, Lukin M, Cirac J I and Zoller P 2001 *Nature* **414** 413–8

[104] Harel G, Kurizki G, McIver J K and Coutsias E 1996 *Phys. Rev.* A **53** 4534–8

[105] Kurizki G, Bertet P, Kubo Y, Mølmer K, Petrosyan D, Rabl P and Schmiedmayer J 2015 *Proc. Natl Acad. Sci.* 112 3866–73

[106] Haroche S and Raimond J M 2006 Exploring the Quantum: Atoms *Cavities, and Photons* (*Oxford Graduate Texts*) (New York: Oxford University Press)

[107] Álvarez G A, Rao D D B, Frydman L and Kurizki G 2010 *Phys. Rev. Lett.* **105** 160401

[108] Bhaktavatsala Rao D D, Bar-Gill N and Kurizki G 2011 *Phys. Rev. Lett.* **106** 010404

[109] Bar-Gill N, Bhaktavatsala Rao D D and Kurizki G 2011 *Phys. Rev. Lett.* **107** 010404

[110] Sørensen A and Mølmer K 2000 *Phys. Rev.* A **62** 022311

[111] Myatt C J, King B E, Turchette Q A, Sackett C A, Kielpinski D, Itano W M, Monroe C and Wineland D J 2000 *Nature* **403** 269–73

[112] Lin Y, Gaebler J, Reiter F, Tan T R, Bowler R, Sørensen A, Leibfried D and Wineland D 2013 *Nature* **504** 415–8

[113] Julsgaard B, Kozhekin A and Polzik E S 2001 *Nature* **413** 400–3

[114] Lehmberg R H 1970 *Phys. Rev.* A **2** 883–8

[115] Lehmberg R H 1970 *Phys. Rev.* A **2** 889–96

[116] Douglas J S, Habibian H, Hung C L, Gorshkov A, Kimble H J and Chang D 2015 *Nat. Photonics* **9** 326–31

[117] Shahmoon E and Kurizki G 2014 *Phys. Rev.* A **89** 043419

[118] Craig D P and Thirunamachandran T 1984 *Molecular Quantum Electrodynamics* (London: Academic)

[119] Milonni P W 1993 *The Quantum Vacuum: An Introduction to Quantum Electrodynamics* (London: Academic)

[120] Shahmoon E 2015 Van der waals and casimir-polder dispersion forces *Forces of the Quantum Vacuum: An Introduction to Casimir Physics* ed W Simpson and U Leonhardt (Singapore: World Scientific)

[121] Rodriguez A W, Capasso F and Johnson S G 2011 *Nat. Photonics* **5** 211–21

[122] Landauer R 1961 *IBM J. Res. Dev.* **5** 183–91

[123] Szilard L 1929 *Zeitschrift fuer Physik* **53** 840–56 ISSN 0044-3328

[124] Alicki R 1979 *J. Phys. A: Math. Gen.* **12** L103

[125] Lindblad G 1983 Non-Equilibrium Entropy and Irreversibility (Dordrecht: D Reidel)

[126] Gelbwaser-Klimovsky D, Erez N, Alicki R and Kurizki G 2013 *Phys. Rev.* A **88** 022112

[127] Alicki R, Gelbwaser-Klimovsky D and Kurizki G 2012 *ArXiv e-prints* 1205.4552

[128] Gelbwaser-Klimovsky D and Kurizki G 2015 *Sci. Rep.* **5** 7809

[129] Gelbwaser-Klimovsky D and Kurizki G 2014 *Phys. Rev.* E **90** 022102

[130] Geva E and Kosloff R 1992 *J. Chem. Phys.* **97** 4398–412

[131] Kosloff R 2013 *Entropy* **15** 2100–28

[132] Kofman A G, Kurizki G and Sherman B 1994 *J. Mod. Opt.* **41** 353–84